Contrib Mineral Petrol (2017) 172:35
DOI 10.1007/s00410-017-1347-z

ORIGINAL PAPER

A petrological and geochemical study on time-series samples from Klyuchevskoy volcano, Kamchatka arc

Olga Bergal-Kuvikas[1,2,3] · Mitsuhiro Nakagawa[1] · Takeshi Kuritani[1] · Yaroslav Muravyev[2] · Nataliya Malik[2] · Elena Klimenko[2] · Mizuho Amma-Miyasaka[1] · Akiko Matsumoto[1] · Shunjiro Shimada[1]

Received: 5 August 2016 / Accepted: 5 March 2017
© Springer-Verlag Berlin Heidelberg 2017

Abstract To understand the generation and evolution of mafic magmas from Klyuchevskoy volcano in the Kamchatka arc, which is one of the most active arc volcanoes on Earth, a petrological and geochemical study was carried out on time-series samples from the volcano. The eruptive products show significant variations in their whole-rock compositions (52.0–55.5 wt.% SiO_2), and they have been divided into high-Mg basalts and high-Al andesites. In the high-Mg basalts, lower-K and higher-K primitive samples (>9 wt.% MgO) are present, and their petrological features indicate that they may represent primary or near-primary magmas. Slab-derived fluids that induced generation of the lower-K basaltic magmas were less enriched in melt component than those associated with the higher-K basaltic magmas, and the fluids are likely to have been released from the subducting slab at shallower levels for the lower-K basaltic magmas than for higher-K basaltic magmas. Analyses using multicomponent thermodynamics indicates that the lower-K primary magma was generated by ~13% melting of a source mantle with ~0.7 wt.% H_2O at 1245–1260 °C and ~1.9 GPa. During most of the evolution of the volcano, the lower-K basaltic magmas were dominant; the higher-K primitive magma first appeared in AD 1932. In AD 1937–1938, both the lower-K and higher-K primitive magmas erupted, which implies that the two types of primary magmas were present simultaneously and independently beneath the volcano. The higher-K basaltic magmas evolved progressively into high-Al andesite magmas in a magma chamber in the middle crust from AD 1932 to ~AD 1960. Since then, relatively primitive magma has been injected continuously into the magma chamber, which has resulted in the systematic increase of the MgO contents of erupted materials with ages from ~AD 1960 to present.

Keywords Primary magma · Magma generation · Kamchatka arc · Water content · Slab-derived fluids

Introduction

Eruptive materials from polygenetic volcanoes commonly show significant geochemical variation through time. These temporal variations have been examined to understand the underlying magmatic processes for many volcanoes in various tectonic settings (e.g., Garcia et al. 2000; Rizzo et al. 2006; Vlastélic et al. 2005; Matsumoto and Nakagawa 2010), and such information is important for the prediction of future volcanic activities. However, determining the origin of temporal variation is challenging, because such variation reflects the integration of many processes and factors, such as temporal change in the influx of slab-derived fluids into the melting region (for arc volcanoes), progressive melting of the source mantle, and temporal variation in the relative roles of magmatic processes in an evolving magma

Communicated by Timothy L. Grove.

Electronic supplementary material The online version of this article (doi:10.1007/s00410-017-1347-z) contains supplementary material, which is available to authorized users.

✉ Mitsuhiro Nakagawa
mnakagawa@sci.hokudai.ac.jp

[1] Graduate School of Science, Hokkaido University, Sapporo 060-0810, Japan

[2] Institute of Volcanology and Seismology, Far Eastern Branch of Russian Academy of Science, Petropavlovsk-Kamchatsky, Russia 683006

[3] Present Address: Earth Observatory of Singapore, Nanyang Technological University, Singapore 639798, Singapore

Published online: 11 April 2017

chamber, including magma recharge, magma discharge, fractional crystallization, and crustal assimilation.

In this study, we investigated the origin of temporal geochemical variations of erupted materials from Klyuchevskoy volcano in the Kamchatka arc. This volcano is known to be one of the most active arc volcanoes in the world; it has erupted frequently, even within the last 10 years: AD 2007, 2008–2009, 2009–2010, 2011, 2012–2013, 2013, 2015, and 2015–present. The volcano is also characterized by underlying subduction of the Hawaiian–Emperor seamount chain. Therefore, a high flux of slab-derived fluids from the thickened oceanic crust has been proposed as the cause of the exceptional magma productivity of this volcano (Dorendorf et al. 2000). Portnyagin et al. (2005) suggested an additional role of mantle upwelling associated with detachment of a subducted slab fragment. Because of interest in the remarkable magma production rate of this volcano, many petrological and geochemical studies have been carried out (e.g., Khubunaya et al. 1993; Kersting and Arculus 1995; Dorendorf et al. 2000; Ozerov 2000; Churikova et al. 2001; Auer et al. 2009; Mironov and Portnyagin 2011; Kayzar et al. 2014). Most of these studies have divided the eruptive products into "high-Mg basalts" and "high-Al andesites", and the genetic relationship between these two types of magma has been discussed. Although some researchers have contended that the high-Al andesitic magma may have been derived from the high-Mg basaltic magma (e.g., Ariskin et al. 1995; Kersting and Arculus 1995; Khubunaya and Sobolev 1998; Ozerov 2000; Mironov et al. 2001), others have attributed the difference in the geochemical features of the two magmas to source mantle processes (e.g., Dosseto et al. 2003; Auer et al. 2009). To understand the origin and evolutionary history of Klyuchevskoy volcano, it is essential to elucidate the genetic relationships of the different types of magma with distinct geochemical features.

In this study, we obtained high-quality geochemical data of time-series samples (from ~3500 BP to AD 2013) from the volcano. We demonstrate that there must have been at least two different kinds of primary magmas with distinct K_2O contents, and on this basis, we discuss the origin of the temporal variation of the magma compositions, particularly for historical volcanic activities.

Klyuchevskoy volcano

The Kamchatka arc is located at the northeastern convergent boundary of the Eurasian and Pacific plates, below which the Pacific plate is presently being subducted at a rate of ~8 cm/year (Bird 2002). Volcanic activities on Kamchatka date back to the Cretaceous Period. The current plate-tectonic configuration, however, formed in the Late Miocene to Early Pliocene (Dorendorf et al. 2000; Churikova et al. 2001; Avdeiko et al. 2006). The present volcanism is concentrated in three zones subparallel to the trench: the Eastern Volcanic Front (EVF), Central Kamchatka Depression (CKD), and Sredinny Range (SR), from east to west (Fig. 1). The depths to the subducting slab at the EVF, CKD, and SR are 100–140, 100–200, and 300–400 km, respectively (Gorbatov et al. 1997).

The Klyuchevskoy Group, located in the CKD, contains 12 volcanoes including Klyuchevskoy, all younger than ~70 ka and located on Pleistocene plateau basalts and shield volcanoes (e.g., Melekestsev et al. 1991). The magma productivity of the CKD volcanoes during historical times has been as high as 60–90 million tons/year (e.g., Khrenov et al. 1991; Fedotov et al. 2010). The heat flow of the CKD has been estimated as >80 mW/m^2, which is significantly higher than those of the other areas of Kamchatka (e.g., Smirnov and Sugrobov 1980). These geophysical observations and the voluminous volcanism have been attributed to the following complex geodynamic settings and associated processes: (1) the arc–arc junction between the Kuril–Kamchatka arc and the Aleutian arc; (2) opening of a slab window (Yogodzinski et al. 2001); (3) detachment of fragments from the subducted Pacific plate (Levin et al. 2002); (4) slab-edge heating in the mantle wedge due to decreasing thickness of the Pacific plate to the north of the Emperor faults (Davaille and Lees 2004; Portnyagin and Manea 2008); and (5) active rifting in the CKD area (Gontovaya et al. 2010).

Klyuchevskoy volcano (4750 m) is composed mainly of basaltic and basaltic–andesitic lava flows and pyroclastic deposits (Fig. 2). The volcano has developed on the extinct Kamen and Ploskie Sopky volcanoes over the last 7000 years to form a main stratovolcano. There have also been numerous flank eruptions (Fig. 2) since 3500 BP (Braitseva et al. 1995). Most of the associated cinder cones are concentrated on the eastern slope of the volcano and are located along the extension of a regional fault. The first historical record of Klyuchevskoy eruptions dates to AD 1697. After this time, until AD 1932, volcanic activities were concentrated at the top of the volcano. Then, flank eruptions restarted, and formed cinder cones on the lower slopes of the volcano (Menyailov 1947; Tokarev 1990), while summit activities continued. Since the paroxysmal eruption of AD 1993–1994, volcanic activities have been concentrated at the top of the volcano.

Analytical methods

In this study, as a Japanese–Russian joint research project on Klyuchevskoy volcano from 2010 to 2014, we collected ~250 samples with eruption ages that span from

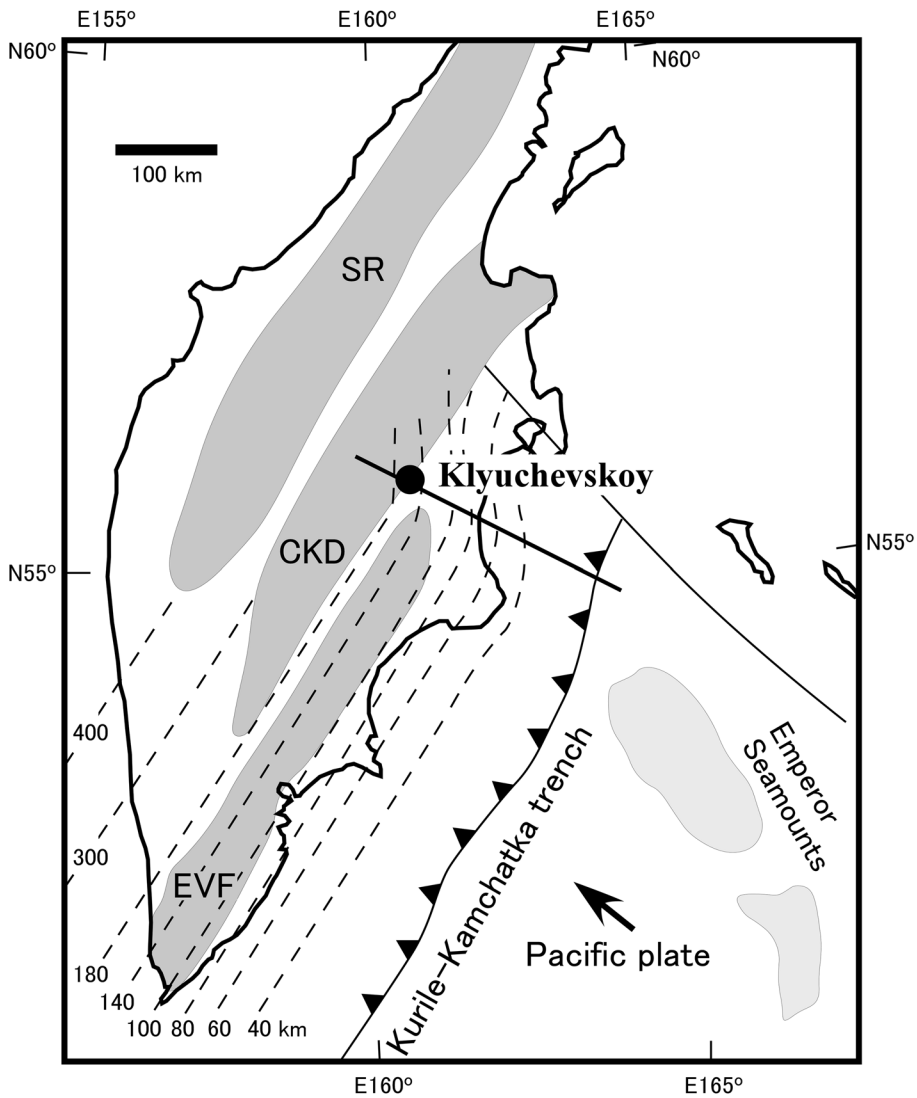

Fig. 1 Map showing the location of Klyuchevskoy volcano. Present volcanism is concentrated in three zones subparallel to the trench: the Eastern Volcanic Front (EVF), Central Kamchatka Depression (CKD), and Sredinny Range (SR), from east to west. The distributions of these volcanic areas and the depth to the Wadati–Benioff zone are from Auer et al. (2009); the latter is originally from Gorbatov et al. (1997). A *thick bold line* indicates the location of the cross section, as shown in Fig. 11

~3500 BP to AD 2013. The sampling localities are shown in Fig. 2. For whole-rock analysis, rock specimens were crushed to coarse chips with diameters of 3–5 mm. The chips were then rinsed with deionized water in an ultrasonic bath and subsequently dried at 100 °C for >12 h. The washed chips were ground using an agate mill. Concentrations of major elements and some trace elements (Sc, V, Cr, Co, Ni, Rb, Sr, Y, Zr, and Ba) were measured with X-ray fluorescence spectrometry (XRF), using a Spectoris MagiX PRO at the Graduate School of Science, Hokkaido University. For the XRF analysis, powdered samples were kept at 900 °C for >12 h in a muffle furnace, and glass beads were prepared via fusion with an alkali flux (2-to-1 sample dilution) consisting of a 4-to-1 mixture of lithium tetraborate and lithium metaborate. Concentrations of additional trace elements were determined for selected samples via inductively coupled plasma mass spectrometry (ICP–MS), using a Thermo Fisher Scientific X-series device.

The analytical procedures followed for chemical separation were based on the methods of Pin et al. (1994) and Noguchi et al. (2011) for Sr, Pin et al. (1994) and Pin and Zalduegui (1997) for Nd, and Kuritani and Nakamura (2002) for Pb. Isotopic ratios were determined with a multiple collector (MC)–ICP–MS (Neptune Plus, Thermo Fisher Scientific) at the Graduate School of Science, Hokkaido University. Mass fractionation factors for Sr and Nd were internally corrected using $^{86}Sr/^{88}Sr = 0.1194$ and $^{146}Nd/^{144}Nd = 0.7219$, respectively, and those for Pb were corrected using Tl as an external standard. In addition, the obtained data were corrected by applying a standard bracketing method using NIST987, JNdi-1, and NIST981 for the Sr, Nd, and Pb isotopic analyses, respectively. Finally, the corrected data were normalized to $^{87}Sr/^{86}Sr = 0.710214$ for NIST 987, $^{143}Nd/^{144}Nd = 0.512117$ for JNdi-1, and $^{206}Pb/^{204}Pb = 16.9424$, $^{207}Pb/^{204}Pb = 15.5003$, and

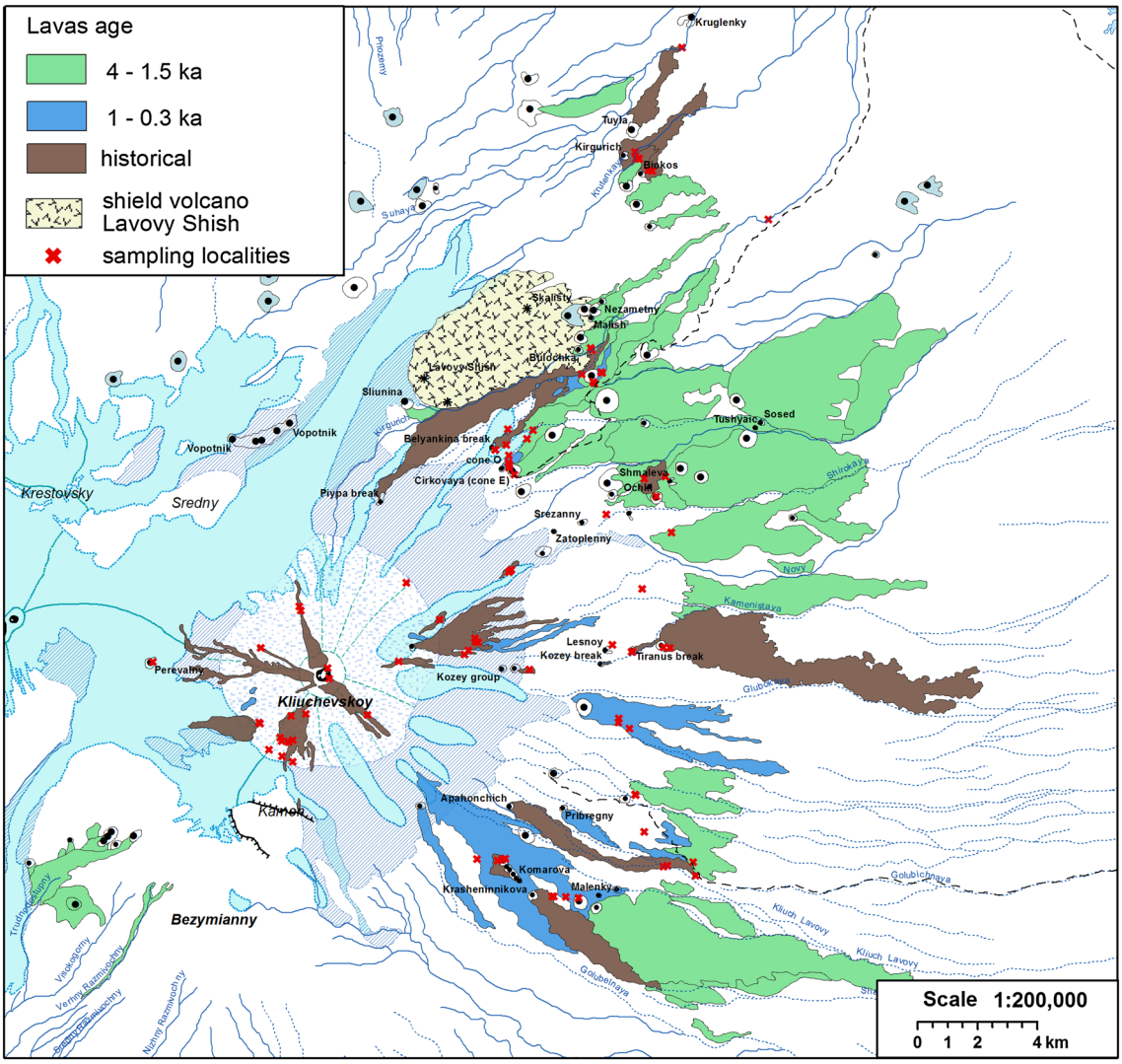

Fig. 2 Geological map of Klyuchevskoy volcano, showing the sampling localities. This map was modified after Khrenov et al. (1991)

$^{208}Pb/^{204}Pb = 36.7266$ for NIST981 (Kuritani and Nakamura 2003). The results of replicate analyses of the major and trace element compositions and Sr, Nd, and Pb isotopic ratios of the Geological Survey of Japan reference material JB-3 measured during the course of this study, as well as the reference values, are provided by Kuritani et al. (2017).

Mineral compositions were determined using a JEOL JXA-8800 electron microprobe at the Graduate School of Science, Hokkaido University. For mafic minerals, an accelerating voltage of 15 kV, a beam current of 20 nA, and a counting time of 20 s were adopted. Operating conditions for plagioclase were an accelerating voltage of 15 kV and a beam current of 10 nA with a counting time of 10 s and a beam diameter of 10 μm. Both oxide and natural mineral standards were used, and data were obtained using the ZAF correction method.

Petrography and mineral chemistry

Lavas and scoria from the volcano have mainly basaltic and basaltic-andesitic compositions. As shown in the following, the whole-rock MgO contents of the studied samples range from ~4 to ~12 wt.%. The phenocryst assemblages of primitive samples (>~9 wt.% MgO) are typically characterized by olivine and clinopyroxene, and those of the other samples are composed of plagioclase, olivine, clinopyroxene, and rare orthopyroxene. Fe–Ti oxide minerals are also observed as accessory phases. Some rocks contain mantle xenoliths that consist of olivine, clinopyroxene, and orthopyroxene. The phenocryst contents are variable, from ~5 to ~25 vol.%.

The chemical compositions of representative olivine, pyroxene, and plagioclase phenocrysts are listed in Table A1. The olivine phenocrysts typically show normal

zoning in terms of Mg# [$100 \times Mg/(Mg + Fe^{2+})$]. The Mg# values of the cores of the olivine phenocrysts in the Klyuchevskoy samples fall within the range of 65–91. Those in the primitive samples (>9 wt.% MgO) are within 80–91 (Fig. 3a, c) and those in the evolved samples (<6 wt.% MgO) are typically within 65–80 (Fig. 3e). In some samples, the Mg# values show bimodal distribution; one mode is within 70–80 and the other is within 80–90. The olivine phenocrysts with Mg# >~88 occur as isolated grains, and those with lower Mg# values occasionally form crystal aggregates with other mineral phases. The Mg# values of the cores of the clinopyroxene phenocrysts

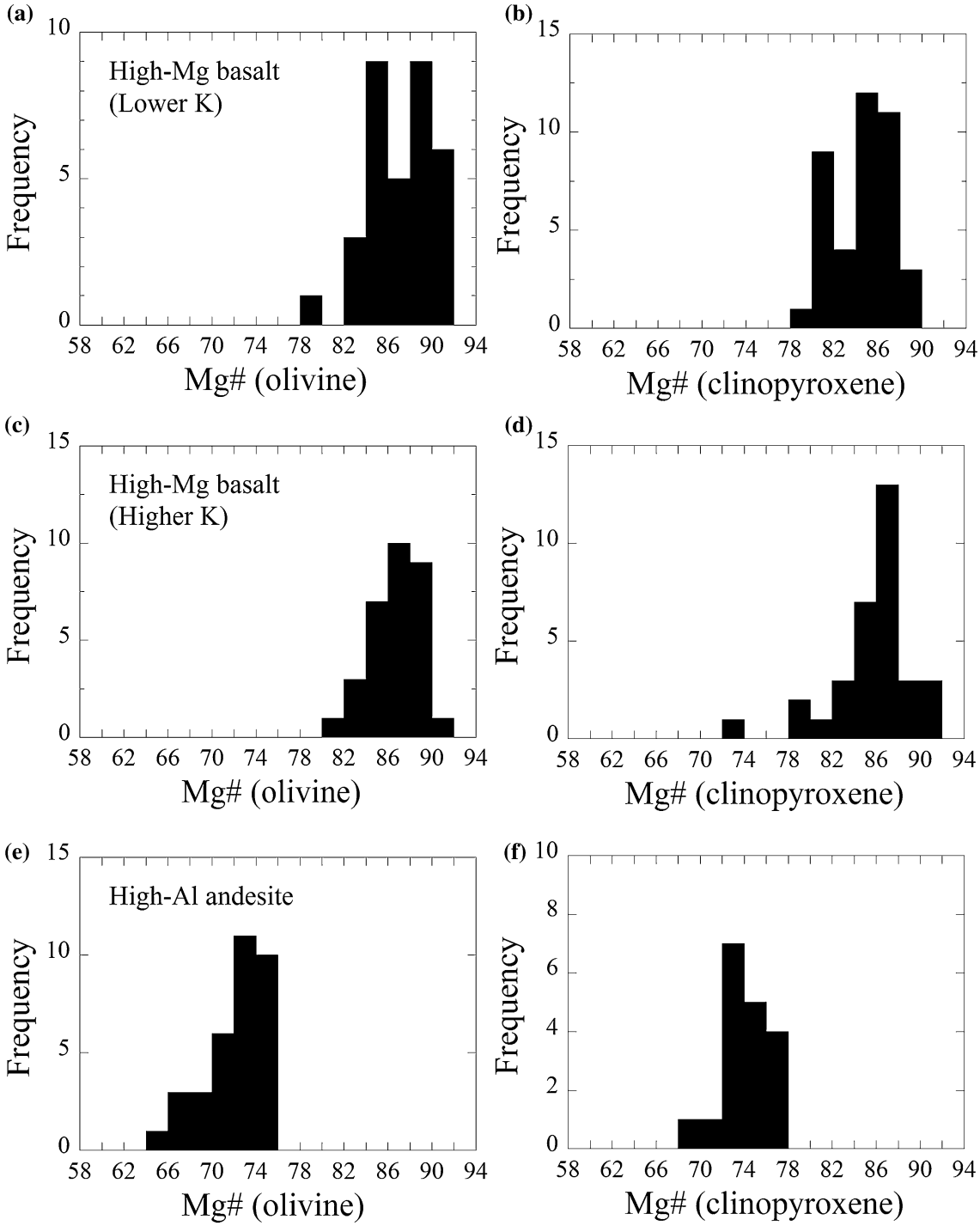

Fig. 3 Histograms of the Mg# values of the cores of olivine and clinopyroxene phenocrysts in a lower-K primitive sample (12Ky-2-1; **a** and **b**), a higher-K primitive sample (12Ky-13-1; **c** and **d**), and a high-Al andesitic sample (11Ky-16-2; **e** and **f**)

commonly range from ~70 to ~90. For the olivine phenocrysts, Mg# values show systematic variation with the whole-rock MgO contents of the samples; those of the primitive samples are within 75–90 (Fig. 3b, d) and those of the evolved samples are within ~70–85 (Fig. 3f). The plagioclase phenocrysts are typically homogeneous with respect to An content [100 × Ca/(Ca + Na)], but phenocrysts with reverse zoning are also present. The An contents of the phenocryst cores are typically within the range of 50–88.

Whole-rock composition

Whole-rock major and trace element compositions of the samples, determined using XRF, are listed in Table 1 and Table A2. MgO variation diagrams for SiO_2, Al_2O_3, Fe_2O_3, and K_2O are displayed in Fig. 4, and those for Ni, Y, Zr, and Ba are shown in Fig. 5. The samples show significant variation in SiO_2 content (52–55 wt.%). As reported in previous studies (e.g., Kersting and Arculus 1995; Ozerov 2000), the products have a compositional range from high MgO–low Al_2O_3 to low MgO–high Al_2O_3 (Fig. 4b). On this basis, the compositions are divided into high-Mg basalts (>~7 wt.% MgO) and high-Al andesites (<~7 wt.% MgO) according to the classification of previous studies. The MgO-rich samples are characterized by high CaO and Ni and low SiO_2, K_2O, Y, Zr, and Ba contents. The older samples (4–1.5 ka) have relatively high MgO and low SiO_2 contents, whereas the historical samples (younger than AD 1932) have relatively low MgO and high SiO_2 contents. It is noteworthy that two kinds of high-Mg basaltic samples are observed with distinct K_2O contents; those from the Bulochka vent (2650 years BP; Auer et al. 2009) with lower K_2O content (~0.6 wt.%) and those from the Tuyla vent (AD 1932 products) with higher K_2O content (~0.9 wt.%) (Fig. 4d). In this study, the high-Mg basaltic samples were further divided into lower-K basalts (<0.8 wt.% K_2O) and higher-K basalts (>0.8 wt.% K_2O). The compositions of the historical eruption products show temporal variations (Fig. 6). The K_2O and MgO contents tend to increase and decrease, respectively, with decreasing eruption ages from AD 1932 to ~AD 1950, and the K_2O and MgO contents decrease and increase, respectively, from AD 1950 to the present.

Trace element concentrations determined using ICP-MS and Sr, Nd, and Pb isotopic compositions of representative samples are listed in Table 1 and Table A2. A primitive mantle-normalized multi-element diagram for the representative samples (most magnesian samples in the individual eruption stages) is shown in Fig. 7. The patterns for the Klyuchevskoy samples are characterized by negative anomalies of Nb and Ta, and positive spikes in Sr, which are characteristics of subduction-zone magmas. The trace element concentrations of the Mg-rich samples are lower than those of the Mg-poor (SiO_2- and Al_2O_3-rich) samples. Variations in the isotopic compositions of Sr, Nd, and Pb with MgO content are shown in Fig. 8a–c. The MgO-rich (SiO_2-poor) samples have relatively low $^{87}Sr/^{86}Sr$ and $^{206}Pb/^{204}Pb$ ratios compared with the MgO-poor samples, whereas the $^{143}Nd/^{144}Nd$ ratios of the MgO-rich samples are similar to those of the MgO-poor samples, with some exceptions. The $^{206}Pb/^{204}Pb$ ratios tend to decrease with eruption ages from AD 1932 to ~1950 (Fig. 6c). Figure 8d–f shows the isotopic data plotted in $^{143}Nd/^{144}Nd$–$^{87}Sr/^{86}Sr$, $^{207}Pb/^{204}Pb$–$^{206}Pb/^{204}Pb$, and $^{208}Pb/^{204}Pb$–$^{206}Pb/^{204}Pb$ diagrams. In the $^{207}Pb/^{204}Pb$–$^{206}Pb/^{204}Pb$ and $^{208}Pb/^{204}Pb$–$^{206}Pb/^{204}Pb$ diagrams, the data primarily show a linear trend, but this trend appears to consist of two sub-trends with slightly different slopes; the trends with higher $^{206}Pb/^{204}Pb$ ratios (>18.29) and those with lower $^{206}Pb/^{204}Pb$ ratios (<18.29) consisting mainly of 4–1.5 ka samples.

Compositional diversity of the Klyuchevskoy magmas

The Klyuchevskoy samples show considerable compositional variation, ranging from ~12 to ~4 wt.% in MgO. This compositional diversity may have resulted from heterogeneity of the primary magmas, as well as from differentiation processes, such as fractional crystallization, crustal assimilation, and magma mixing. As described above, two kinds of primitive magmas with distinct K_2O contents are present: those from the Bulochka vent with lower K_2O content (2650 years BP) and those from the Tuyla vent with higher K_2O content (AD 1932) (Fig. 4d). The significant difference in K_2O contents within the MgO content range of 8–9 wt.% may indicate that the higher-K primitive magma could not have been derived from the lower-K primitive magma through fractional crystallization. Therefore, it can be inferred that the lower-K and higher-K primitive magmas were derived from different source mantle materials.

As shown in Fig. 6, the historical magmas tend to evolve systematically from AD 1932 to ~1960, with a few exceptional samples (AD 1937–1938) with significantly low K_2O and high MgO contents. By applying the two-pyroxene geobarometer of Putirka (2008) to the cpx–opx pairs in the AD 1937–1938 sample (11Ky102-1), a crystallization pressure of 0.4 GPa was determined. This observation may indicate that the primitive higher-K magma with ~0.9 wt.% K_2O evolved into the andesitic magma with ~1.2 wt.% K_2O over ~30 years in a middle crustal magma chamber. In addition, the $^{206}Pb/^{204}Pb$ ratios decrease systematically from 18.30 to 18.29 with decreasing eruption ages after AD 1932 to ~1960 (Fig. 6c), which implies that assimilation of crustal materials occurred simultaneously with fractional crystallization. Kayzar et al. (2014) reported that middle and lower crustal xenoliths from Bezymianny volcano, which is located 9 km from

Table 1 Whole-rock compositions of the representative samples from Klyuchevskoy volcano

Sample name	12Ky7-2	12Ky2-1	Ky10-14	12Ky13-1	11Ky108-1	Ky10-5	11Ky16-2	11Ky103-4	12Ky103-1	13Ky11o
Latitude (N)	56º08′45″	56º09′10″'	56º06′56″	56º12′43″	56º03′41″	56º59′47″	55º59′58″	56º05′13″	56º02′12″	56º03′15″
Longitude (E)	160º47′47″	160º47′30″	160º44′54″	160º49′04″	160º48′32″	160º49′23″	160º44′03″	160º44′43″	160º37′24″	160º38′23″
Age	4–1.5 ka	4–1.5 ka	1–0.5 ka	AD 1932	AD 1937–1938	AD 1946	AD 1956	AD 1980	AD 1994	AD 2013
Major elements, wt%										
SiO_2	53.50	50.86	52.80	52.42	53.14	54.09	53.91	53.44	53.04	52.69
TiO_2	1.01	0.80	0.91	0.87	0.95	1.07	1.15	1.12	1.14	1.08
Al_2O_3	17.12	13.16	16.33	14.09	15.79	17.15	18.50	17.52	17.80	16.74
Fe_2O_3*	9.17	9.52	9.59	9.23	9.55	9.21	9.00	9.44	9.51	9.66
MnO	0.16	0.17	0.16	0.17	0.17	0.16	0.15	0.17	0.17	0.17
MgO	5.47	11.25	7.86	9.14	6.95	5.68	4.34	5.23	4.78	5.43
CaO	8.34	10.01	9.36	9.48	9.10	8.60	7.94	8.41	8.21	8.53
Na_2O	3.45	2.35	3.00	2.70	3.04	3.35	3.67	3.41	3.45	3.28
K_2O	0.93	0.56	0.65	0.87	0.92	1.06	1.17	1.03	1.02	0.95
P_2O_5	0.19	0.13	0.15	0.16	0.18	0.21	0.22	0.20	0.20	0.19
Total	99.34	98.81	100.80	99.12	99.80	100.58	100.06	99.96	99.31	98.72
Trace elements (XRF), ppm										
Sc	29.6	38.5	32.3	38.1	34.2	31.4	22.8	28.6	29.8	27.7
V	246	242	253	247	258	273	273	274	273	264
Cr	93.0	757.9	236.4	527.7	186.9	85.8	26.7	48.1	22.9	72.0
Co	31.7	41.0	35.9	35.7	34.3	33.3	29.9	33.0	31.5	32.3
Ni	34.2	184.9	83.6	133.6	54.5	32.7	24.2	30.3	24.4	30.3
Rb	17.2	10.9	13.0	15.4	15.0	17.4	19.3	17.5	17.2	16.0
Sr	331	239	311	310	326	364	397	360	357	323
Y	22.7	17.0	21.1	19.4	21.8	22.6	23.4	24.7	24.9	24.9
Zr	89.0	60.7	69.5	69.4	78.0	86.9	96.1	90.4	91.1	88.3
Ba	383	215	232	302	334	372	420	398	412	404
Trace elements (ICP-MS), ppm										
Nb	1.8	1.3	1.5	1.5	1.7	2.2	2.0	2.1	1.5	1.9
Cs	0.4	0.2	0.4	0.4	0.5	0.4	0.5	0.5	0.5	0.4
La	6.9	4.0	5.2	5.7	6.4	7.9	7.5	7.2	7.2	6.8
Ce	16.9	10.9	13.2	14.0	15.6	19.1	18.3	18.6	17.7	16.9
Pr	2.7	1.7	2.1	2.2	2.4	3.0	2.9	2.8	2.8	2.7
Nd	12.7	8.4	10.2	10.3	11.7	14.3	13.6	13.4	13.5	13.0
Sm	3.6	2.4	2.9	2.9	3.2	3.8	3.7	3.7	3.8	3.6

Table 1 (continued)

Trace elements (ICP-MS), ppm										
Eu	1.1	0.8	1.0	0.9	1.0	1.2	1.2	1.2	1.2	1.2
Gd	3.8	2.9	3.2	3.2	3.6	4.1	4.1	4.2	4.2	4.1
Tb	0.7	0.5	0.6	0.5	0.6	0.7	0.7	0.7	0.7	0.7
Dy	3.9	3.0	3.4	3.2	3.7	4.1	4.1	4.2	4.2	4.2
Ho	0.9	0.6	0.7	0.7	0.8	0.9	0.9	0.9	0.9	0.9
Er	2.4	1.8	2.1	2.0	2.3	2.5	2.4	2.6	2.6	2.6
Tm	0.4	0.3	0.3	0.3	0.3	0.4	0.4	0.4	0.4	0.4
Yb	2.3	1.7	2.0	1.9	2.2	2.3	2.3	2.4	2.4	2.5
Lu	0.3	0.3	0.3	0.3	0.3	0.4	0.4	0.4	0.4	0.4
Hf	2.4	1.6	2.0	1.9	2.2	2.6	2.6	2.5	2.4	2.4
Ta	0.1	0.1	0.1	0.1	0.1	0.1	0.1	0.1	0.1	0.1
Th	1.0	0.4	0.5	0.8	0.7	0.9	0.9	0.8	0.8	0.9
U	0.6	0.3	0.4	0.4	0.4	0.5	0.5	0.5	0.5	0.5
Isotopes										
$^{87}Sr/^{86}Sr$	0.703644	0.703525	0.703485	0.703528	0.703499	0.703595	0.703617	0.703594	0.703622	0.703636
2 SE	0.000011	0.000011	0.000009	0.000014	0.000008	0.000009	0.000008	0.000009	0.000008	0.000010
$^{143}Nd/^{144}Nd$	0.513097	0.513101	0.513046	0.513091	0.513102	0.513113	0.513097	0.513100	0.513071	0.513096
2 SE	0.000005	0.000007	0.000005	0.000010	0.000006	0.000006	0.000009	0.000005	0.000009	0.000009
$^{206}Pb/^{204}Pb$	18.3006	18.2862	18.2740	18.3026	18.2969	18.2987	18.2896	18.3040	18.3122	18.3166
2 SE	0.0005	0.0003	0.0007	0.0003	0.0011	0.0008	0.0007	0.0005	0.0009	0.0007
$^{207}Pb/^{204}Pb$	15.4946	15.4911	15.4852	15.4932	15.4915	15.4916	15.4886	15.4944	15.4956	15.4975
2 SE	0.0004	0.0003	0.0006	0.0003	0.0009	0.0008	0.0006	0.0005	0.0009	0.0006
$^{208}Pb/^{204}Pb$	37.9628	37.9503	37.9077	37.9543	37.9424	37.9384	37.9289	37.9580	37.9685	37.9810
2 SE	0.0015	0.0009	0.0017	0.0009	0.0028	0.0021	0.0018	0.0014	0.0022	0.0018

*Total Fe as Fe_2O_3

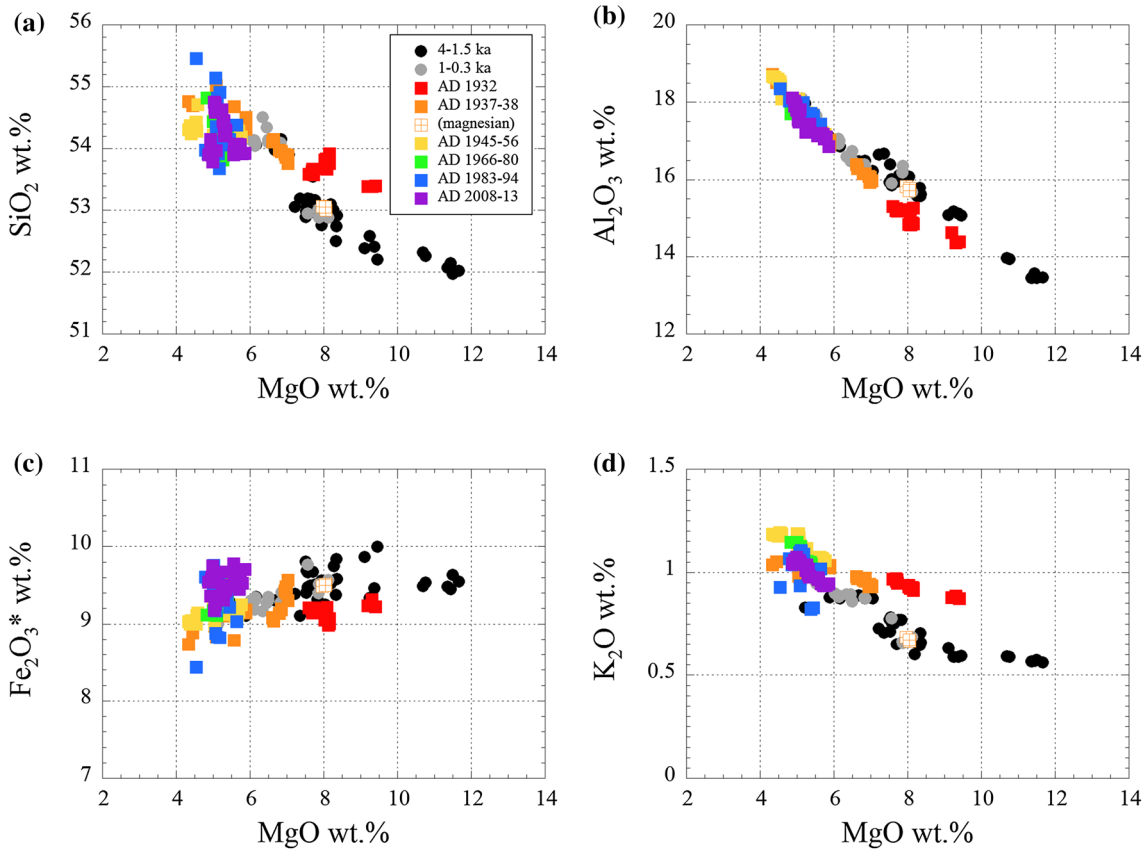

Fig. 4 MgO variation diagrams for SiO_2, Al_2O_3, Fe_2O_3*, and K_2O contents of samples from Klyuchevskoy volcano

Klyuchevskoy volcano, have less radiogenic Pb isotopic compositions ($^{206}Pb/^{204}Pb = 18.18–18.23$) than do the historical products of Klyuchevskoy volcano. This observation is consistent with decrease of the $^{206}Pb/^{204}Pb$ ratios of the magmas through progressive assimilation and fractional crystallization.

Figure 6d also shows the temporal variation of $\delta^{18}O$ values of olivine phenocrysts for the historical products (Dorendorf et al. 2000; Auer et al. 2009). The $\delta^{18}O$ values appear to increase significantly with decreasing eruption ages after AD 1932 to ~1960. The products of Klyuchevskoy volcano are known to have unusually high $\delta^{18}O$ values. However, the source of these high $\delta^{18}O$ values has been a matter of debate; various possible source, such as fluids from subducted sediments, fluids from the subducted Hawaii-Emperor Seamounts, a pyroxenite mantle source, metasomatized lithospheric and/or asthenospheric mantle, and hydrothermally altered crust, have been examined (e.g., Pineau et al. 1999; Pokrovsky and Volynets 1999; Dorendorf et al. 2000; Bindeman et al. 2004; Auer et al. 2009). The observed temporal variation of the $\delta^{18}O$ values (Fig. 6d) may indicate that the high $\delta^{18}O$ values of the Klyuchevskoy products are partly attributed to the assimilation of crustal materials. However, this inference does not rule out the possibility that the high-$\delta^{18}O$ materials also reside in the mantle, because the primitive lower-K (Bulochka cone) and higher-K (Tuyla cone) products have significantly higher $\delta^{18}O$ values than those typical of the mantle (Dorendorf et al. 2000; Auer et al. 2009).

The MgO contents and K_2O contents of the products tend to increase and decrease, respectively, with decreasing eruption ages after ~AD 1960 (Fig. 6a, b). This observation may indicate that relatively primitive magma has been injected continuously into the middle crustal magma chamber. It is noteworthy that the $^{206}Pb/^{204}Pb$ isotopic ratios of the products also increase systematically with decreasing eruption ages from ~AD 1960 to the present, with some exception samples, and that those of the products formed after AD 2000 (>18.31; Fig. 6c) are higher than those of any other products of the volcano (<~18.30; Fig. 8c). Therefore, this higher-$^{206}Pb/^{204}Pb$ primitive magma may represent a new type of primary magma that was not produced beneath Klyuchevskoy volcano previously.

High-Al andesites (<~7 wt.% MgO) occurred throughout the evolution of the volcano (Fig. 6), and their origin has been a matter of debate (e.g., Kersting and Arculus 1995; Ariskin et al. 1995; Khubunaya and Sobolev 1998; Ozerov 2000; Mironov et al. 2001; Dosseto et al.

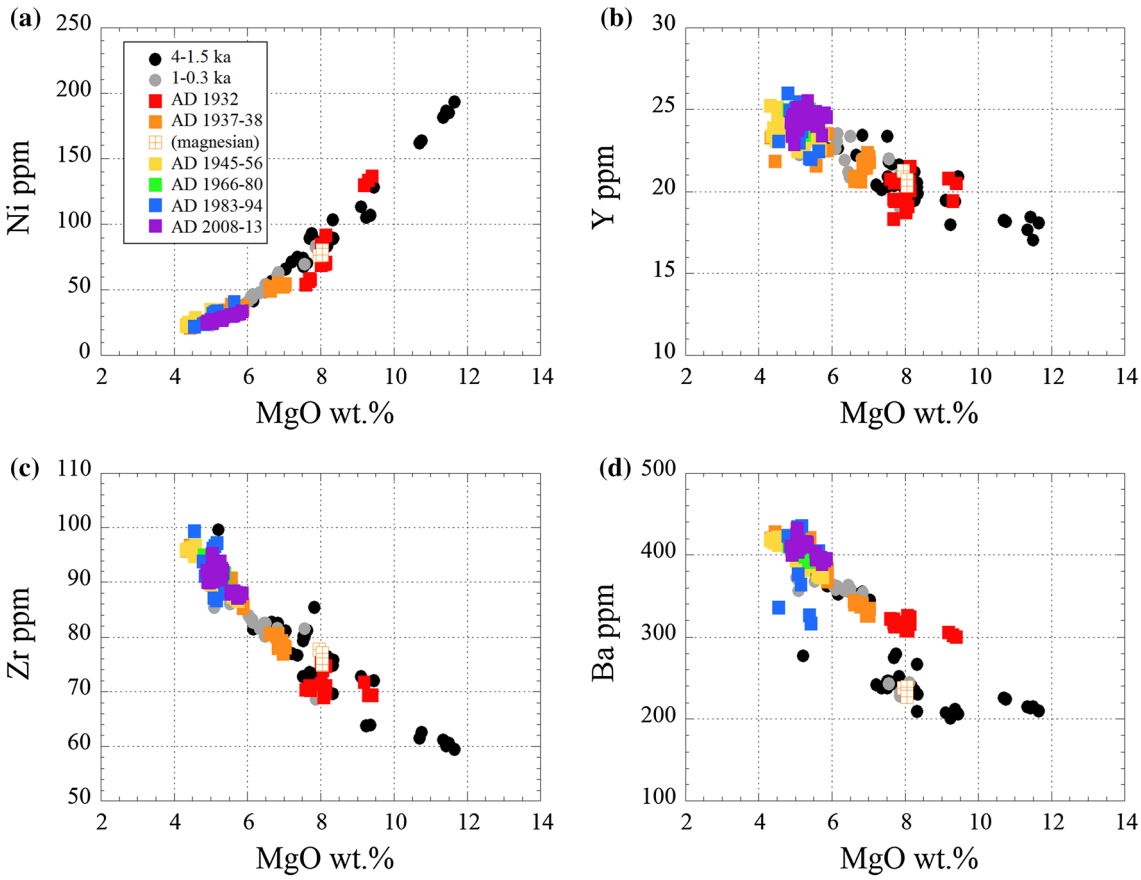

Fig. 5 MgO variation diagrams for Ni, Y, Zr, and Ba contents of samples from Klyuchevskoy volcano

2003; Auer et al. 2009). This study shows that the high-Al andesites of the historical eruptions originated primarily from assimilation and fractional crystallization of the higher-K basaltic magmas.

Origin of lower-K and higher-K basaltic magmas

The lower-K and higher-K primitive magmas are inferred to have been derived from different source mantle materials, as discussed above, and the MgO contents of the most magnesian lower-K and higher-K basaltic samples (12Ky2-2 and 12Ky13-2) are 11.7 and 9.4 wt.%, respectively; these samples may represent primary or near-primary magmas. The compositions of the primary magmas are controlled mainly by parameters, such as the degree of melting of the source mantle, the compositions of the slab-derived fluids, and the mixing ratios between the slab-derived fluids and the source mantle (e.g., Kimura et al. 2009). With these factors, the degree of melting alone cannot explain the difference between the lower-K and higher-K primary magmas, because the isotopic ratios of the two primary magmas differ (Fig. 8).

Figure 9 shows a Th/Yb–Ba/La diagram in which the compositions of the primitive (>9 wt.% MgO) lower-K and higher-K samples, as well as that of the depleted mid-ocean ridge basalt source mantle (DMM) (Salter and Stracke 2004), are plotted. Trace element ratios, such as Th/Yb and Ba/La, have been widely used to identify the nature of slab-derived fluids (e.g., Hawkesworth et al. 1991; Pearce and Peate 1995). Because Ba is soluble in slab-derived aqueous fluids, and because La, Yb, and Th are immobile in these aqueous fluids, the addition of the fluids to the mantle results in high Ba/La and low Th/Yb ratios of the partial melts. However, because sediments have high Th/Yb and low Ba/La ratios, the partial melt is characterized by high Th/Yb and low Ba/La ratios from the addition of the melt component to the mantle.

In the figure, partial melts of the DMM have Th/Yb and Ba/La ratios similar to those of the DMM, because Th, Yb, Ba, and La are all incompatible elements. The Th/Yb and Ba/La ratios of both the lower-K and higher-K primary magmas which are different from those of the DMM, which may indicate that these magmas were produced through mixing of the DMM component and slab-derived fluids with distinct Th/Yb and Ba/La ratios. In addition,

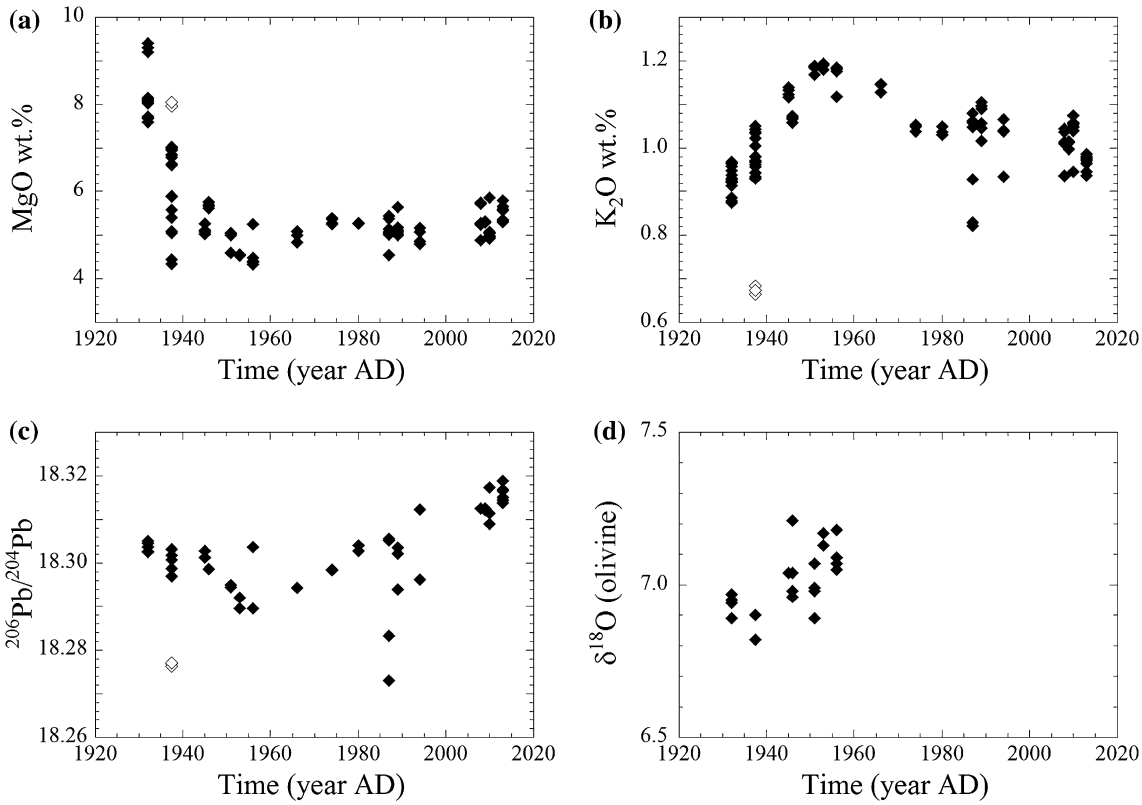

Fig. 6 Temporal variation of MgO and K_2O contents, $^{206}Pb/^{204}Pb$ ratios, and $\delta^{18}O$ values of the historical Klyuchevskoy samples. The $\delta^{18}O$ data are taken from Dorendorf et al. (2000) and Auer et al. (2009)

the lower-K magmas and the higher-K magmas do not lie along the same line from the DMM. This observation implies that the compositions of the slab-derived fluids associated with the lower-K primary magma differed from those of the higher-K primary magma. Both the lower-K and higher-K primary magmas have relatively high Th/Yb and Ba/La ratios. Therefore, the slab-derived fluids are suggested to have been supercritical liquids, in which both Ba and Th are soluble (Kessel et al. 2005). The involvement of supercritical liquids in the source mantle beneath Klyuchevskoy has previously been suggested by Portnyagin et al. (2007). The proportion of the melt-like component in supercritical liquids tends to increase with the slab depth from which the liquids were derived (Kessel et al. 2005). Therefore, the slab-derived fluids of the higher-K primary magma may have been derived from greater depth levels than were those of the lower-K primary magma.

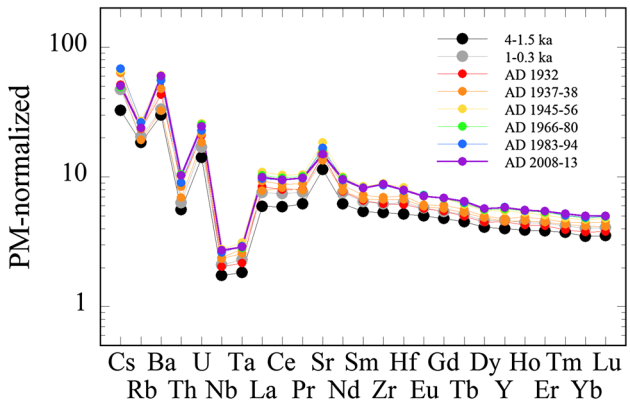

Fig. 7 Primitive mantle–normalized multi-element concentration diagram for representative samples of Klyuchevskoy volcano. Trace element concentrations of the primitive mantle are taken from Sun and McDonough (1989)

Conditions of magma generation

For the primitive lower-K basalts from the Bulochka vent, water contents in the melt were determined by Auer et al. (2009). They reported 0.4–3.9 wt.% H_2O for glass inclusions in a primitive basaltic scoria sample (KLV 5/8; 11.3 wt.% MgO), which had a whole-rock major element composition that was generally similar to that of sample 12Ky2-2 in this study. Given that the inclusions with the highest water contents (3.9 wt.%) were those least affected by degassing, the H_2O/K_2O ratio of the glass was determined to be 9.3. This ratio is within the range of 7–11

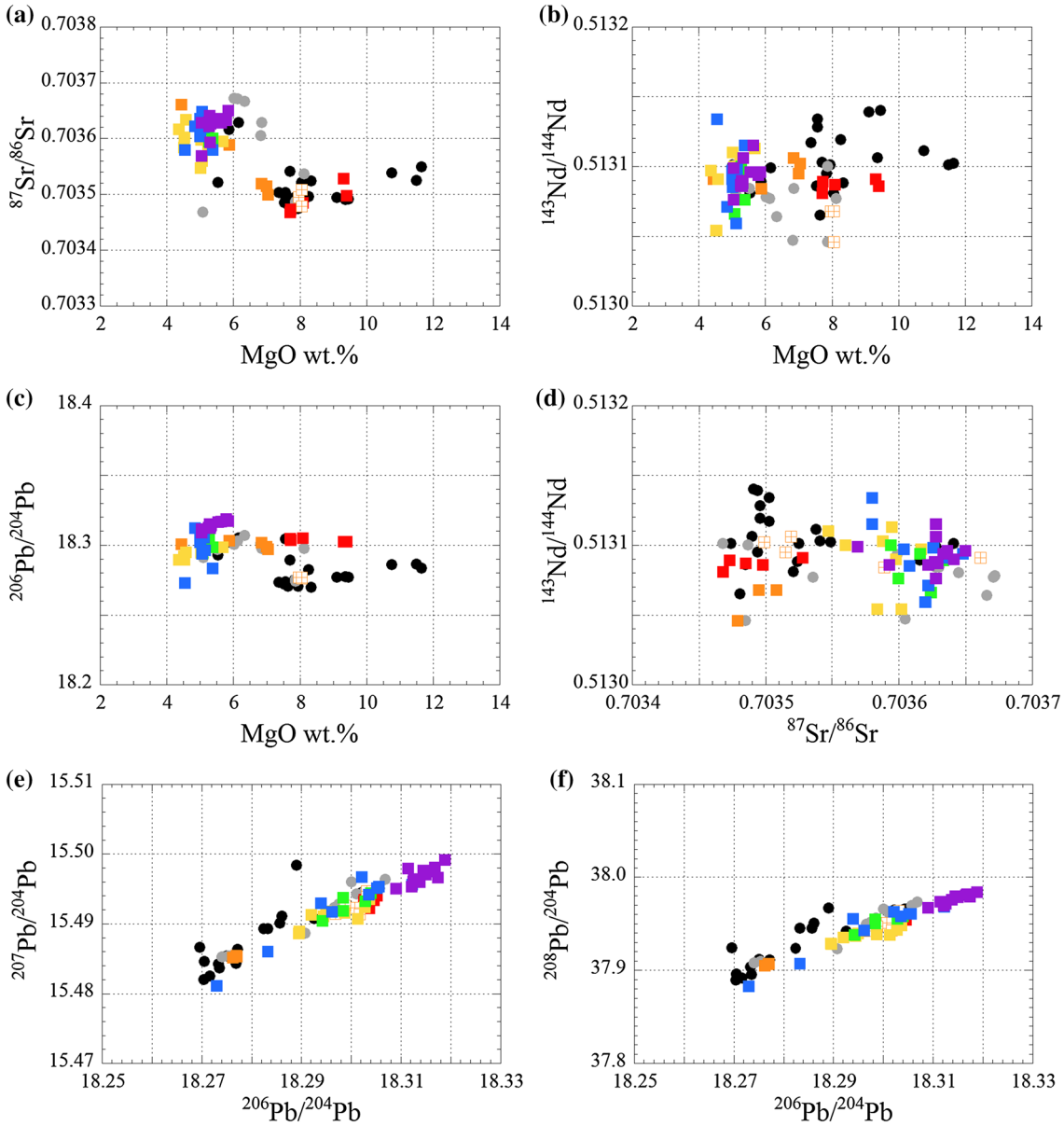

Fig. 8 MgO variation diagrams for $^{87}Sr/^{86}Sr$, $^{143}Nd/^{144}Nd$, and $^{208}Pb/^{204}Pb$ and Sr, Nd, and Pb isotopic compositions shown in $^{143}Nd/^{144}Nd$ versus $^{87}Sr/^{86}Sr$, $^{207}Pb/^{204}Pb$ versus $^{206}Pb/^{204}Pb$, and $^{208}Pb/^{204}Pb$ versus $^{206}Pb/^{204}Pb$ diagrams for samples from Klyuchevskoy volcano. The legend is the same, as shown in Fig. 5

determined recently for glass inclusions in lavas from the Bulochka vent by Mironov et al. (2015). Analytical errors for water content analysis using FT–IR may be as high as 10% (e.g., Roggensack et al. 1997). Assuming that the H_2O/K_2O ratio did not change significantly during magmatic differentiation, the H_2O content of the melt with the composition of 12Ky2-2 was found to be 5.1 ± 0.5 wt.% using the K_2O content of 0.55 wt.% of the sample. The alphaMELTS model in the MELTS mode (Ghiorso and Sack 1995; Asimow and Ghiorso 1998; Smith and Asimow 2005) with the oxygen fugacity of Ni-NiO buffer indicated that the 12Ky2-2 melt with 5.1 wt.% H_2O (the most primitive lower-K basalt sample) was in equilibrium with olivine with Mg#90.5. This observation indicates that the composition of 12Ky13-2 may actually represent a primary magma composition.

The degrees of melting of the DMM were estimated for the lower-K primary magma based on the distribution of Ti between the source mantle and melt following the method of Kelley et al. (2006). Using the bulk distribution coefficient for Ti of 0.04 and a TiO_2 content of the DMM of 0.133 wt.% (Salters and Stracke 2004), as well as the TiO_2

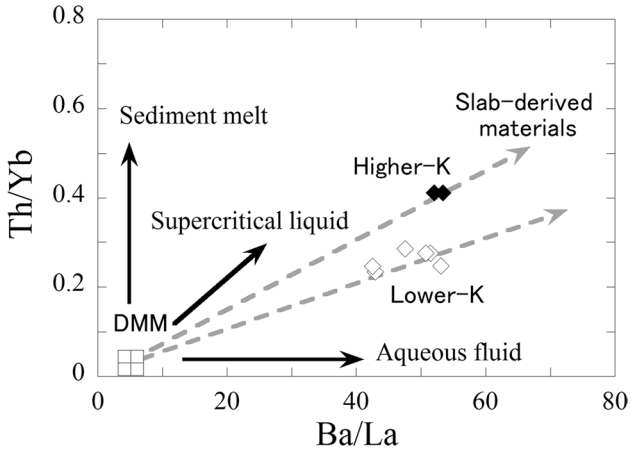

Fig. 9 Th/Yb and Ba/La diagram showing the compositions of the primary lower-K and primary higher-K magmas, as well as those of the DMM. The compositions of the DMM are from Salter and Stracke (2004)

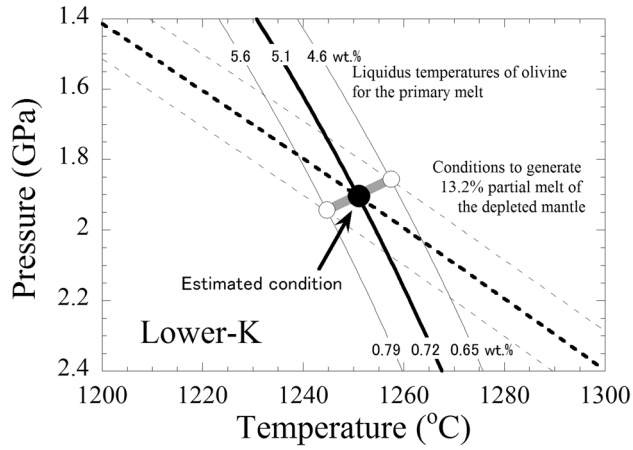

Fig. 10 Estimated conditions of magma generation for the lower-K primitive magma. The P–T conditions of the source mantle required to generate 13.2% partial melt with a source water content of 0.72 ± 0.07 wt.%, calculated using the parameterized hydrous mantle melting model of Katz et al. (2003), and the liquidus temperature of olivine for a primary magma with a water content of 5.1 ± 0.5 wt.%, calculated using the alphaMELTS model in pMELTS mode (Asimow and Ghiorso 1998; Smith and Asimow 2005) and the model for the effect of water on the lowering of olivine liquidus temperatures for primitive melts (Médard and Grove 2008), are shown as *dashed lines* and *continuous lines*, respectively. *Thick gray lines* indicate the possible P–T condition of the magma generation

content of 12Ky2-2 (Table 1), a degree of melting of 13.2% was determined. In this case, the water content of the source mantle was calculated to be 0.72 ± 0.07 wt.% using Eq. 10 of Kelley et al. (2006).

The temperature and pressure conditions of magma generation were estimated following a similar method to that of Kuritani and Nakagawa (2016) using two constraints: (1) the primary magma was generated through 13.2% melting of the DMM and (2) the primary magma was in equilibrium with olivine in the source mantle. First, the pressure and temperature conditions required to generate a 13.2% partial melt of the DMM were calculated for a source water content of 0.72 ± 0.07 wt.% using the parameterized hydrous mantle melting model of Katz et al. (2003); the result is shown in Fig. 10. It has been suggested that the pMELTS model underestimates the effect of H_2O on the lowering of the olivine liquidus temperature for primitive melts (e.g., Médard and Grove 2008). Therefore, the liquidus temperature of olivine for the dry primary melt was calculated using the alphaMELTS model in the pMELTS mode (Ghiorso et al. 2002; Smith and Asimow 2005), and the effect of water on the lowering of the olivine liquidus temperature was then corrected using the model of Médard and Grove (2008). The calculated olivine liquidus temperature for the primary melt with 5.1 ± 0.5 wt.% H_2O in temperature–pressure space is shown in Fig. 10. The temperature and pressure conditions for the magma that satisfy the 13.2% degree of melting of the DMM and the equilibration of the melt with olivine in the source mantle were constrained to 1245–1260 °C and ~1.9 GPa, respectively.

For the primitive higher-K basalts from the Tuyla vent, Mironov and Portnyagin (2011) reported 0.06–0.08 wt.% H_2O for glass inclusions in olivine phenocrysts. However, these low water contents are interpreted to have resulted from water loss from the inclusions during eruption and subsequent cooling (Mironov and Portnyagin 2011). A hygrometer, such as that based on plagioclase-melt thermodynamic equilibrium (e.g., Putirka 2008), may be used to estimate water contents in melt. However, at Klyuchevskoy volcano, plagioclase appears in a crystallization phase only in evolved andesitic samples. Therefore, it is not possible to reliably estimate the conditions of magma generation for the higher-K basalts.

Comparison with geophysical study

Recently, Koulakov et al. (2016) investigated the 3D velocity structure beneath Klyuchevskoy volcano in detail, and suggested that slab-derived fluids are released from the subducting slab at variable depths (Fig. 11). As shown in Fig. 6, the relatively primitive (>8 wt.% MgO) higher-K and lower-K basaltic magmas erupted in AD 1932 and AD 1937–1938 (open diamonds in Fig. 6), respectively. This observation may indicate that the primary higher-K and lower-K magmas were probably generated simultaneously and independently in the upper mantle beneath the volcano. If this was the case, the slab-derived fluids for the lower-K magma and the higher-K magma may have been derived from the slab at depths of 70–90 km and >90 km, respectively (Fig. 11). We suggest that the lower-K basaltic

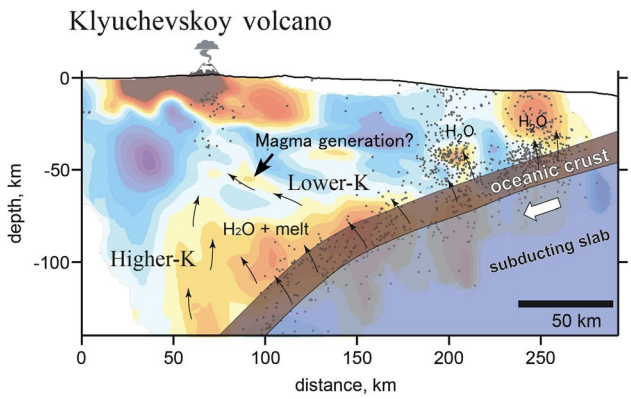

Fig. 11 Vertical cross section of S-wave velocity along the profile indicated in Fig. 1 (modified from Koulakov et al. 2016). Areas indicated with "Lower-K" and "Higher-K" show possible sites of fluid flows from the subducting slab for the generation of the lower-K and higher-K primary magmas, respectively

magmas were generated at 1245–1260 °C and ~1.9 GPa. Therefore, the region with a relatively low-Vs anomaly at 60–70 km depths may represent the generation site (Fig. 11), given that the lower-K primitive magmas erupted at AD 1937–1938 were generated under similar conditions to those of the lower-K products from the Bulochka vent.

Conclusions

To understand the generation and evolution of magmas at Klyuchevskoy volcano, we carried out a petrological and geochemical study on basalts and basaltic andesites from the volcano and reached the following conclusions:

1. There have been two different kinds of primitive magmas with distinct K_2O contents. The lower-K basalts have been dominant throughout the evolution of the volcano, whereas the eruption of the higher-K primitive basalts was limited mostly to AD 1932.
2. The lower-K and higher-K primary magmas were generated by influxes of different slab-derived fluids into the melting region. The slab-derived fluids of the higher-K magmas are inferred to have contained larger amounts of a sediment component than those of the lower-K magmas. Therefore, the slab-derived fluids of the higher-K primary magma may have been derived from deeper levels than those of the lower-K primary magma.
3. The H_2O content of the lower-K primary magma was estimated to be ~5.1 wt.% based on water content analysis of glass inclusions by Auer et al. (2009). Thermodynamic analyses have indicated that the lower-K primary magma was generated by ~13% melting of the source mantle with ~0.7 wt.% H_2O at 1245–1260 °C and ~1.9 GPa.
4. The appearance of the higher-K basaltic magmatism at AD 1932 resulted from an influx of a new batch of slab-derived fluids into the melting region. We suggest that lower-K and higher-K primitive magmas were present simultaneously and independently in the upper mantle beneath the volcano in AD 1937–1938.
5. The higher-K basaltic magmas evolved progressively into high-Al andesitic magmas in a magma chamber in the middle crust through assimilation and fractional crystallization from AD 1932 to ~AD 1950. Relatively primitive magma has then been injected continuously into the magma chamber from AD 1950 to present. Therefore, the high-Al andesitic magmatism of the volcano was partly the result of assimilation and fractional crystallization of the high-Mg basalt magmas.

Acknowledgements We are grateful to Y. Ishizuka, T. Hasegawa, S. Uesawa, S. Serovetnikov, S. Chirkov and colleagues from the Institute of Volcanology and Seismology, Kamchatka for supporting us in field work at Klyuchevskoy volcano. Editorial handling by T. L. Grove and constructive review and fruitful comments by M. Portnyagin and R. Arculus are greatly appreciated. We thank all the members of the Petrology and Volcanology Group at Hokkaido University for productive discussions and technical assistance. This work was supported by a research Grant for a Japan–Russia joint research project funded by the JSPS and RFBR Grant number 14-05-92108 and by a research grant from the JSPS KAKENHI Grant number 16H04071 for T.K. and 22253005 for M.N. B.-K. O. is grateful to the Japanese government for the opportunity to study at Hokkaido University (Monbukagakusho MEXT scholarship, 2010–2015).

References

Ariskin AA, Barmina GS, Ozerov AY, Nielsen RL (1995) Genesis of high-alumina basalts from Kluchevskoi volcano. Petrology 3:496–521

Asimow PD, Ghiorso MS (1998) Algorithmic modifications extending MELTS to calculate subsolidus phase relations. Am Miner 83:1127–1132

Auer S, Bindeman I, Wallace P, Ponomareva V, Portnyagin M (2009) The origin of hydrous, high-$\delta^{18}O$ voluminous volcanism: diverse oxygen isotope values and high magmatic water contents within the volcanic record of Klyuchevskoy volcano, Kamchatka, Russia. Contrib Miner Petrol 157:209–230

Avdeiko GP, Palueva AA, Khleborodova OA (2006) Geodynamic conditions of volcanism and magma formation in the Kurile–Kamchatka island-arc system. Petrology 14:230–246

Bindeman IN, Ponomareva VV, Bailey JC, Valley JW (2004) Volcanic arc of Kamchatka: a province with high-$\delta^{18}O$ magma sources and large-scale $^{18}O/^{16}O$ depletion of the upper crust. Geochim Cosmochim Acta 68:841–865. doi:10.1016/j.gca.2003.07.009

Bird P (2002) An updated digital model of plate boundaries. Geochem Geophys Geosyst doi:10.1029/2001GC000252

Braitseva OA, Melekestsev IV, Ponomareva VV, Sulerzhitsky LD (1995) Ages of calderas, large explosive craters and active volcanoes in the Kuril-Kamchatka region, Russia. Bull Volcanol 57:383–402

Churikova T, Dorendorf F, Wörner G (2001) Sources and fluids in the mantle wedge below Kamchatka, evidence from across-arc geochemical variation. J Petrol 42:1567–1593

Davaille A, Lees JM (2004) Thermal modeling of subducted plates: tear and hotspot at the Kamchatka corner. Earth Planet Sci Lett 226:293–304

Dorendorf F, Wiechert U, Wörner G (2000) Hydrated sub-arc mantle: a source for the Kluchevskoy volcano, Kamchatka/Russia. Earth Planet Sci Lett 175:69–86

Dosseto A, Bourdon B, Joron JL, Dupré B (2003) U-Th-Pa-Ra study of the Kamchatka arc: new constrains on the genesis of arc lavas. Geochim Cosmochim Acta 67:2857–2877

Fedotov SA, Zharinov NA, Gontovaya LI (2010) The magmatic system of the Klyuchevskaya group of volcanoes inferred from data on its eruptions, earthquakes, deformation, and deep structure. J Volcanol Seism 4:1–33

Garcia MO, Pietruszka AJ, Rhodes JM, Swanson K (2000) Magmatic processes during the prolonged Pu'u 'O'o eruption of Kilauea volcano, Hawaii. J Petrol 41:967–990

Ghiorso M, Sack RO (1995) Chemical mass transfer in magmatic processes IV. A revised and internally consistent thermodynamic model for the interpolation and extrapolation of liquid–solid equilibria in magmatic systems at elevated temperatures and pressures. Contrib Miner Petrol 119:197–212

Ghiorso MS, Hirschmann MM, Reiners PW, Kress VC (2002) The pMELTS: a revision of MELTS for improved calculation of phase relations and major element partitioning related to partial melting of the mantle to 3 GPa. Geochem Geophys Geosyst 3:2001GC000217

Gontovaya LI, Popruzhenko SV, Nizkous IV (2010) Upper mantle structure in the ocean-continent transition zone: Kamchatka. J Volcanol Seismol 4:232–247

Gorbatov A, Kostoglodov V, Suárez G, Gordeev E (1997) Seismicity and structure of the Kamchatka subduction zone. J Geophys Res 102:17883–17898

Hawkesworth CJ, Hergt JM, Ellam RM, McDermott F (1991) Element fluxes associated with subduction related magmatism. Philos Trans R Soc A 335:393–405

Katz RF, Spiegelman M, Langmuir CH (2003) A new parameterization of hydrous mantle melting. Geochem Geophys Geosyst doi: 10.1029/2002GC000433

Kayzar TM, Nelson BK, Bachmann O, Bauer AM, Izbekov PE (2014) Deciphering petrogenic processes using Pb isotope ratios from time-series samples at Bezymianny and Klyuchevskoy volcanoes, central Kamchatka depression. Contrib Mineral Petrol 168:1067

Kelley KA, Plank T, Grove TL, Stolper EM, Newman S, Hauri E (2006) Mantle melting as a function of water content beneath back-arc basins. J Geophys Res 111:B09208

Kersting AB, Arculus RJ (1995) Pb isotope composition of Klyuchevskoy volcano, Kamchatka and North Pacific sediments: implications for magma genesis and crustal recycling in the Kamchatka arc. Earth Planet Sci Lett 136:133–148

Kessel R, Schmidt MW, Ulmer P, Pettke T (2005) Trace element signature of subduction-zone fluids, melts and supercritical liquids at 120–180 km depth. Nature 437:724–727

Khrenov AP, Dvigalo VN, Kirsanov IT, Fedotov SA, Gorel'chik VI, Zharinov NA (1991) Klyuchevskoy volcano. Active volcanoes of Kamchatka 1:146–163 (in Russian)

Khubunaya SA, Sobolev AV (1998) Primary melts of calc-alkaline magnesian basalts of Klyuchevskoy volcano, Kamchatka. Dokl Rus Acad Sci 360:100–102 (in Russian)

Khubunaya SA, Bogoyavlenskii SO, Novgorodtseva TY, Okrugina AI (1993) Mineralogical features of magnesian basalts as a reflection of fractionation in the magma chamber of Klyuchevskoi Volcano. Vulkanol Seism 3:46–68 (**Russian**)

Kimura J-I, Hacker BR, van Keken PE, Kawabata H, Yoshida T, Stern RJ (2009) Arc Basalt Simulator version 2, a simulation for slab dehydration and fluid-fluxed mantle melting for arc basalts: modeling scheme and application. Geochem Geophys Geosys doi: 10.1029/2008GC002217

Koulakov IY, Kukarina EV, Gordeev EI, Chebrov VN, Vernikovsky VA (2016) Magma sources in the mantle wedge beneath the volcanoes of the Klyuchevskoy group and Kizimen based on seismic tomography modeling. Rus Geol Geophys 57:82–94

Kuritani T, Nakagawa M (2016) Origin of ultra rear-arc magmatism at Rishiri Volcano, Kuril Arc. Geochem Geophys Geosyst doi: 10.1002/2016GC006594

Kuritani T, Nakamura E (2002) Precise isotope analysis of nanogram-level Pb for natural rock samples without use of double spikes. Chem Geol 186:31–43

Kuritani T, Nakamura E (2003) Highly precise and accurate isotopic analysis of small amounts of Pb using ^{205}Pb–^{204}Pb and ^{207}Pb–^{204}Pb, two double spikes. J Anal Atom Spectrom 18:1464–1470

Kuritani T, Sakuyama T, Kamada N, Yokoyama T, Nakagawa M (2017) Fluid-fluxed melting of mantle versus decompression melting of hydrous mantle plume as the cause of intraplate magmatism over a stagnant slab: implications from Fukue Volcano Group, SW Japan. Lithos doi: 10.1016/j.lithos.2017.02.011

Levin V, Shapiro N, Park J, Ritzwoller M (2002) Seismic evidence for catastrophic slab loss beneath Kamchatka. Nature 418:763–767

Lindsley DH (1983) Pyroxene thermometry. Am Miner 68:477–493

Matsumoto A, Nakagawa M (2010) Formation and evolution of silicic magma plumbing system: petrology of the volcanic rocks of Usu volcano, Hokkaido, Japan. J Volcanol Geotherm Res 196:185–207

Médard E, Grove TL (2008) The effect of H_2O on the olivine liquidus of basaltic melts: experiments and thermodynamic models. Contrib Miner Petrol 155:417–432

Melekestsev IV, Khrenov AP, Kozhernyaka NN (1991) Tectonic position and general description of volcanoes of Northern group and Sredinny Range. In: Fedotov SA, Masurenkov YP (eds) Active volcanoes of Kamchatka. Nauka, Moscow, pp 74–81

Menyailov AA (1947) Dynamic and eruptive mechanism of Klyuchevskoy volcano in 1937–1938. Publications of volcanological laboratory and Kamchatka volcanological station 4:90

Mironov NL, Portnyagin MV (2011) H_2O and CO_2 in parental magmas of Kliuchevskoi volcano inferred from study of melt and fluid inclusions in olivine. Russ Geol Geophys 52:1353–1367

Mironov NL, Portnyagin MV, Pletchov PY, Khubunaya SA (2001) Final stages of magma evolution in Klyuchevskoy volcano, Kamchatka: evidence from melt inclusions in minerals of high-alumina basalts. Petrology 9:46–62

Mironov N, Portnyagin M, Botcharnikov R, Gurenko A, Hoernle K, Holtz F (2015) Quantification of the CO_2 budget and H_2O-CO_2 systematics in subduction-zone magmas through experimental hydration of melt inclusions in olivine at high H_2O pressure. Earth Planet Sci Lett 425:1–11

Noguchi T, Shinjo R, Ito M, Takada J, Oomori T (2011) Barite geochemistry from hydrothermal chimneys of the Okinawa Trough: insight into chimney formation and fluid/sediment interaction. J Miner Petrol Sci 106:26–35

Ozerov AY (2000) The evolution of high-alumina basalts of the Klyuchevskoy volcano, Kamchatka, Russia, based on microprobe analyses of mineral inclusions. J Volcanol Geotherm Res 95:65–79

Pearce JA, Peate DW (1995) Tectonic implications of the composition of volcanic arc magmas. Ann Rev Earth Planet Sci 23:251–285

Pin C, Zalduegui JFS (1997) Sequential separation of light rare-earth elements, thorium and uranium by miniaturized extraction chromatography: application to isotopic analyses of silicate rocks. Anal Chimica Acta 339:79–89

Pin C, Briot D, Bassin C, Poitrasson F (1994) Concomitant separation of strontium and samarium-neodymium for isotopic analysis in silicate samples, based on specific extraction chromatography. Anal Chimica Acta 298:209–217

Pineau F, Semet MP, Grassineau N, Okrugin VM, Javoy M (1999) The genesis of the stable isotope (O, H) record in arc magmas: the Kamchatka's case. Chem Geol 153:93–124

Pokrovsky BG, Volynets ON (1999) Oxygen-isotope geochemistry in volcanic rocks of the Kurile–Kamchatka arc. Petrology 7:227–251

Portnyagin M, Manea VC (2008) Mantle temperature control on composition of arc magmas along the Central Kamchatka Depression. Geology 36:519–522

Portnyagin M, Hoernle K, Avdeiko G, Hauff F, Werner R, Bindeman I, Uspensky V, Garbe-Schöenberg D (2005) Transition from arc to oceanic magmatism at the Kamchatka–Aleutian junction. Geology 33:25–28

Portnyagin M, Hoernle K, Plechov P, Mironov N, Khubunaya S (2007) Constraints on mantle melting and composition and nature of slab components in volcanic arcs from volatiles (H_2O, S, Cl, F) and trace elements in melt inclusions from Kamchatka Arc. Earth Planet Sci Lett 255:53–69

Putirka KD (2008) Thermometers and barometers for volcanic systems. Rev Miner Petrol 69:61–120

Rizzo A, Caracausi A, Favara R, Martelli M, Paonita A, Paternoster M, Nuccio PM, Rosciglione A (2006) New insights into magma dynamics during the last two eruptions of Mount Etna as inferred by geochemical monitoring from 2002 to 2005. Geochem Geophys Geosys 7:2005GC001175

Roggensack K, Hervig RL, McKnight SB, Williams SN (1997) Explosive basaltic volcanism from Cerro Negro volcano: influence of volatiles on eruptive style. Science 277:1639–1642

Salters VJM, Stracke A (2004) Composition of the depleted mantle. Geochem Geophys Geosys 5:Q05B07

Smirnov YB, Sugrobov VM (1980) Terrestrial heat flow in the Kurile-Kamchatka and Aleutian provinces, II. The map of measured and background heat flow. Volcanol Seismol 1:16–31

Smith PM, Asimow PD (2005) Adiabat_1ph: a new public front-end to the MELTS, pMELTS, and pHMELTS models. Geochem Geophys Geosys doi: 10.1029/2004GC000816

Sun S–S, McDonough WF (1989) Chemical and isotopic systematics of oceanic basalts: implications for mantle composition and processes. In: Saunders AD, Norry M (eds) Magmatism in the Ocean Basins. Geol Soc London Spec Pub 42:313–345

Tokarev PI (1990) Prediction of Flank Eruptions at Klyuchevskoi volcano. Volcanol Seismol 10:917–943

Vlastélic I, Staudacher T, Semet M (2005) Rapid change of lava composition from 1998 to 2002 at Piton de la Fournaise (Réunion) inferred from Pb isotopes and trace elements; evidence for variable crustal contamination. J Petrol 46:79–107

Yogodzinski GM, Lees JM, Churikova TG, Dorendorf F, Wöerner G, Volynets ON (2001) Geochemical evidence for the melting of subducting oceanic lithosphere at plate edges. Nature 409:500–504